

Theoretical analysis and experimental validation of radial cascaded composite ultrasonic transducer

Xiao-Yu Wang(王晓宇), Zhi-Xin Yu(余芷欣), Jing Hu(胡静), and Shu-Yu Lin(林书玉)
Citation: Chin. Phys. B, 2021, 30 (**4**): 040701. DOI: 10.1088/1674-1056/abd399
Journal homepage: http://cpb.iphy.ac.cn; http://iopscience.iop.org/cpb

What follows is a list of articles you may be interested in

Coupling analysis of transmission lines excited by space electromagnetic fields based on time domain hybrid method using parallel technique

Zhi-Hong Ye(叶志红), Xiao-Lin Wu(吴小林), Yao-Yao Li(李尧尧)
Chin. Phys. B, 2020, 29 (**9**): 090701. DOI: 10.1088/1674-1056/ab96a6

Simulation study of high voltage GaN MISFETs with embedded PN junction

Xin-Xing Fei(费新星), Ying Wang(王颖), Xin Luo(罗昕), Cheng-Hao Yu(于成浩)
Chin. Phys. B, 2020, 29 (**8**): 080701. DOI: 10.1088/1674-1056/ab90f7

Effect of different bending shapes on thermal properties of flexible light-emitting diode filament

Liping Wang(王立平), Wenbo Li(李文博), Yichao Xu(徐一超), Bobo Yang(杨波波), Mingming Shi(石明明), Jun Zou(邹军), Yang Li(李杨), Xinglu Qian(钱幸璐), Fei Zheng(郑飞), Lei Yang(杨磊)
Chin. Phys. B, 2018, 27 (**11**): 110701. DOI: 10.1088/1674-1056/27/11/110701

A slope-based decoupling algorithm to simultaneously control dual deformable mirrors in a woofer-tweeter adaptive optics system

Tao Cheng(程涛), Wenjin Liu(刘文劲), Boqing Pang(庞博清), Ping Yang(杨平), Bing Xu(许冰)
Chin. Phys. B, 2018, 27 (**7**): 070704. DOI: 10.1088/1674-1056/27/7/070704

Theoretical models for designing a 220-GHz folded waveguide backward wave oscillator

Cai Jin-Chi, Hu Lin-Lin, Ma Guo-Wu, Chen Hong-Bin, Jin Xiao, Chen Huai-Bi
Chin. Phys. B, 2015, 24 (**6**): 060701. DOI: 10.1088/1674-1056/24/6/060701

Theoretical analysis and experimental validation of radial cascaded composite ultrasonic transducer*

Xiao-Yu Wang(王晓宇), Zhi-Xin Yu(余芷欣), Jing Hu(胡静)†, and Shu-Yu Lin(林书玉)‡

Shaanxi Key Laboratory of Ultrasonics, Institute of Applied Acoustics, Shaanxi Normal University, Xi'an 710119, *China*

(Received 14 October 2020; revised manuscript received 9 November 2020; accepted manuscript online 15 December 2020)

A radial cascaded composite ultrasonic transducer is analyzed. The transducer consists of three short metal tubes and two radially polarized piezoelectric ceramic short tubes arranged alternately along the radial direction. The short metal tubes and the piezoelectric ceramic short tubes are connected in parallel electrically and in series mechanically, which can multiply the input sound power and sound intensity. Based on the theory of plane stress, the electro-mechanical equivalent circuit of radial vibration of the transducer is derived firstly. The resonance/anti-resonance frequency equation and the expression of the effective electromechanical coupling coefficient are obtained. Excellent electromechanical characteristics are determined by changing the radial geometric dimensions. Two prototypes of the transducers are designed and manufactured to support the analytical theory. It is concluded that the theoretical resonance/anti-resonance frequencies are consistent with the numerical and experimental results. When R_2 is at certain values, both the anti-resonance frequency and effective electromechanical coupling coefficient corresponding to the second mode have maximal values. The radial cascaded composite ultrasonic transducer is expected to be used in the fields of ultrasonic water treatment and underwater acoustics.

Keywords: radial cascaded transducer, radial vibration, equivalent circuit, effective electromechanical coupling coefficient

PACS: 07.07.Mp, 07.05.Tp **DOI:** 10.1088/1674-1056/abd399

1. Introduction

Piezoelectric ultrasonic transducer, an important electro-acoustic conversion device, is used in the ultrasonic cleaning, ultrasonic welding, ultrasonic nondestructive testing, ultrasonic medical imaging, ultrasonic water treatment, underwater acoustic communication and energy collection, etc.[1–8] In the field of power ultrasonic, Langevin ultrasonic transducer,[9–14] as known as longitudinal sandwiched ultrasonic transducer, has been widely used.

In recent years, with the rapid development of power ultrasonic technology, traditional longitudinal sandwiched ultrasonic transducers cannot meet the development needs. Therefore, the optimization of traditional transducers and the development of new models are the research hotspots of scholars. Kim *et al.* developed a flexible piezoelectric composite transducer composed of an active piezoelectric material and a passive polymer matrix.[15] The transducer has achieved excellent flexibility, sensitivity and bandwidth, which is mainly suitable for biomedical and industrial applications. Cannata *et al.*[16] designed, manufactured and tested sensitive wideband lithium niobate ($LiNbO_3$) unit ultrasonic transducers in the 20–80 MHz frequency range. Abdullah *et al.*[17] made an attempt to derive the general principles of the design of a high-power ultrasonic transducer, excited by a DC-biased alternating electrical source. Previously, we proposed tubular ultrasonic vibration systems,[18–21] wherein, equivalent circuits corresponding to various types of radial composite transducers were derived and the vibrational characteristics were analyzed. Li *et al.*[22] proposed a wideband ultrasonic transducer, which is composed of two radial enhanced composite vibrators with different resonance frequencies stacked along the axial direction. Choi developed a negative group delay circuit for high-frequency ultrasonic transducers.[23] On the basis of a typical piezoelectric/elastic sandwich transducer, Wang and Shi[24] designed two models of multilayer piezoelectric/elastic composite cylindrical transducers with radial polarizations and analyzed dynamic characteristics.

In order to improve the power capacity, input sound power, sound intensity and heat dissipation performance of the transducer, a radial cascaded composite ultrasonic transducer is proposed in this paper. Based on the plane stress theory, the equivalent circuit of the transducer is derived and the resonance/antiresonance frequency equation and the expression of the effective electromechanical coupling coefficient are obtained. Ignoring the losses and loads, the vibrational characteristics of the transducer are analyzed theoretically. Two prototypes of the radial cascaded composite ultrasonic transducers are manufactured and tested to verify the correctness of the theoretical results.

*Project supported by the National Natural Science Foundation of China (Grant Nos. 11674206 and 11874253).

†Corresponding author. E-mail: hjwlx@snnu.edu.cn

‡Corresponding author. E-mail: sylin@snnu.edu.cn

© 2021 Chinese Physical Society and IOP Publishing Ltd

2. The electromechanical equivalent circuit of the transducer

The structure and longitudinal profile diagram of the radial cascaded composite ultrasonic transducer are displayed, as shown in Fig. 1. The transducer is composed of three short metal tubes denoted as m_1, m_2, and m_3, and two piezoelectric ceramic short tubes denoted as p_1, p_2, along the radial direction. Two piezoelectric ceramic short tubes are radially polarized shown by the arrows in Fig. 1(b). Three metal short tubes and two piezoelectric ceramic short tubes are connected in parallel electrically and in series mechanically. A cylindrical coordinate system is established, in which r and z are radial and axial coordinates, respectively. The radius of the transducer from inside to outside is R_1, R_2, R_3, R_4, R_5 and R_6, the axial height is h, and the radial dimension is much larger than the height. The direction of the applied excitation field of the transducer is parallel to the direction of polarization.

Combined with the equivalent circuits of a single piezoelectric ceramic short tube and a short metal tube deduced in Ref. [18], the electro-mechanical equivalent circuit of radial cascaded composite ultrasonic transducer can be obtained, as shown in Fig. 2. Here, the forces and displacements are continuous at the contact surface of the metal/piezoelectric tube.

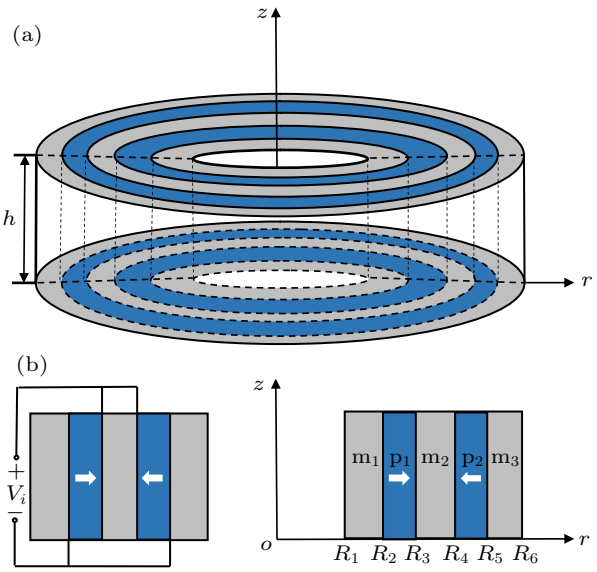


Fig. 1. Radial cascaded composite ultrasonic transducer: (a) structure, (b) longitudinal profile diagram.

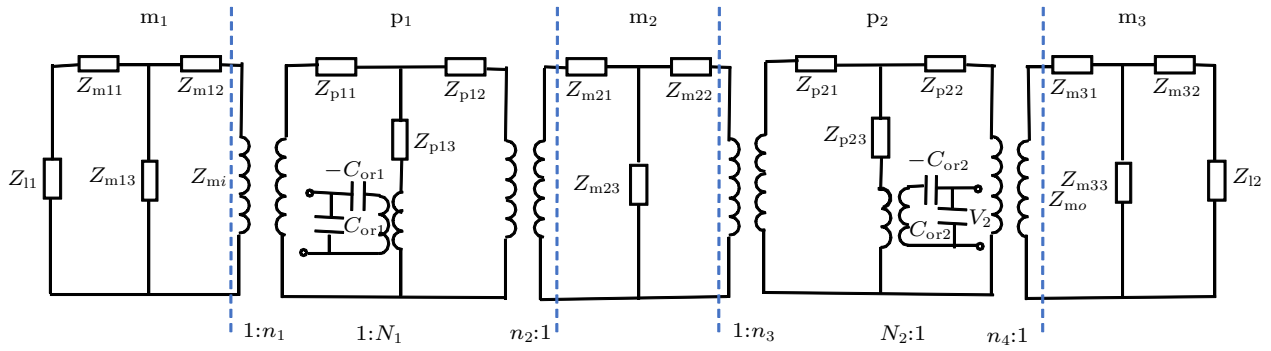


Fig. 2. The electromechanical equivalent circuit of the radial cascaded composite ultrasonic transducer.

In Fig. 2, Z_{l1} and Z_{l2} are the load mechanical resistances of the inner and outer end faces of the transducer, Z_{m11}, Z_{m12}, Z_{m13}, Z_{m21}, Z_{m22}, Z_{m23}, Z_{m31}, Z_{m32}, and Z_{m33} are mechanical impedances of short metal tubes. The expressions of the mechanical impedances of each part are as follows:[18]

$$\begin{aligned} Z_{m11} &= \mathrm{j}\frac{2Z_1}{\pi k_1 R_1\left[\mathrm{J}_1(k_1R_2)\mathrm{Y}_1(k_1R_1)-\mathrm{J}_1(k_1R_1)\mathrm{Y}_1(k_1R_2)\right]} \\ &\quad\times\left[\frac{\mathrm{J}_1(k_1R_2)\mathrm{Y}_0(k_1R_1)-\mathrm{J}_0(k_1R_1)\mathrm{Y}_1(k_1R_2)-\mathrm{J}_1(k_1R_1)\mathrm{Y}_0(k_1R_1)+\mathrm{J}_0(k_1R_1)\mathrm{Y}_1(k_1R_1)}{\mathrm{J}_1(k_1R_1)\mathrm{Y}_0(k_1R_1)-\mathrm{J}_0(k_1R_1)\mathrm{Y}_1(k_1R_1)}\right] \\ &\quad-\mathrm{j}\frac{2Z_1(1-\sigma 1)}{\pi(k_1R_1)^2\left[\mathrm{J}_1(k_1R_1)\mathrm{Y}_0(k_1R_1)-\mathrm{J}_0(k_1R_1)\mathrm{Y}_1(k_1R_1)\right]}, \end{aligned} \tag{1}$$

$$\begin{aligned} Z_{m12} &= \mathrm{j}\frac{2Z_1}{\pi k_1 R_1\left[\mathrm{J}_1(k_1R_2)\mathrm{Y}_1(k_1R_1)-\mathrm{J}_1(k_1R_1)\mathrm{Y}_1(k_1R_2)\right]} \\ &\quad\times\left[\frac{\mathrm{J}_1(k_1R_1)\mathrm{Y}_0(k_1R_2)-\mathrm{J}_0(k_1R_2)\mathrm{Y}_1(k_1R_1)-\mathrm{J}_1(k_1R_2)\mathrm{Y}_0(k_1R_2)+\mathrm{J}_0(k_1R_2)\mathrm{Y}_1(kR_2)}{\mathrm{J}_1(k_1R_2)\mathrm{Y}_0(k_1R_2)-\mathrm{J}_0(k_1R_2)\mathrm{Y}_1(k_1R_2)}\right] \\ &\quad+\mathrm{j}\frac{2Z_2(1-\sigma 1)}{\pi(k_1R_2)^2\left[\mathrm{J}_1(k_1R_2)\mathrm{Y}_0(k_1R_2)-\mathrm{J}_0(k_1R_2)\mathrm{Y}_1(k_1R_2)\right]}, \end{aligned} \tag{2}$$

$$Z_{m13} = \mathrm{j}\frac{2Z_1}{\pi k_1 R_1\left[\mathrm{J}_1(k_1R_2)\mathrm{Y}_1(k_1R_1)-\mathrm{J}_1(k_1R_1)\mathrm{Y}_1(k_1R_2)\right]} = \mathrm{j}\frac{2Z_2}{\pi k_1 R_2\left[\mathrm{J}_1(k_1R_2)\mathrm{Y}_1(k_1R_1)-\mathrm{J}_1(k_1R_1)\mathrm{Y}_1(k_1R_2)\right]}, \tag{3}$$

$$
\begin{aligned}
Z_{\mathrm{m21}} &= \mathrm{j}\frac{2Z_3}{\pi k_2 R_3\left[\mathrm{J}_1(k_2R_4)\mathrm{Y}_1(k_2R_3)-\mathrm{J}_1(k_2R_3)\mathrm{Y}_1(k_2R_4)\right]}\\
&\quad\times\left[\frac{\mathrm{J}_1(k_2R_4)\mathrm{Y}_0(k_2R_3)-\mathrm{J}_0(k_2R_3)\mathrm{Y}_1(k_2R_4)-\mathrm{J}_1(k_2R_3)\mathrm{Y}_0(k_2R_3)+\mathrm{J}_0(k_2R_3)\mathrm{Y}_1(k_2R_3)}{\mathrm{J}_1(k_2R_3)\mathrm{Y}_0(k_2R_3)-\mathrm{J}_0(k_2R_3)\mathrm{Y}_1(k_2R_3)}\right]\\
&\quad-\mathrm{j}\frac{2Z_3(1-\sigma 2)}{\pi(k_2R_3)^2\left[\mathrm{J}_1(k_2R_3)\mathrm{Y}_0(k_2R_3)-\mathrm{J}_0(k_2R_3)\mathrm{Y}_1(k_2R_3)\right]},
\end{aligned}
\tag{4}
$$

$$
\begin{aligned}
Z_{\mathrm{m22}} &= \mathrm{j}\frac{2Z_3}{\pi k_2 R_3\left[\mathrm{J}_1(k_2R_4)\mathrm{Y}_1(k_2R_3)-\mathrm{J}_1(k_2R_3)\mathrm{Y}_1(k_2R_4)\right]}\\
&\quad\times\left[\frac{\mathrm{J}_1(k_2R_3)\mathrm{Y}_0(k_2R_4)-\mathrm{J}_0(k_2R_4)\mathrm{Y}_1(k_2R_3)-\mathrm{J}_1(k_2R_4)\mathrm{Y}_0(k_2R_4)+\mathrm{J}_0(k_2R_4)\mathrm{Y}_1(k_2R_4)}{\mathrm{J}_1(k_2R_4)\mathrm{Y}_0(k_2R_4)-\mathrm{J}_0(k_2R_4)\mathrm{Y}_1(k_2R_4)}\right]\\
&\quad+\mathrm{j}\frac{2Z_4(1-\sigma 2)}{\pi(k_2R_4)^2\left[\mathrm{J}_1(k_2R_4)\mathrm{Y}_0(k_2R_4)-\mathrm{J}_0(k_2R_4)\mathrm{Y}_1(k_2R_4)\right]},
\end{aligned}
\tag{5}
$$

$$
Z_{\mathrm{m23}} = \mathrm{j}\frac{2Z_3}{\pi k_2 R_3\left[\mathrm{J}_1(k_2R_4)\mathrm{Y}_1(k_2R_3)-\mathrm{J}_1(k_2R_3)\mathrm{Y}_1(k_2R_4)\right]} = \mathrm{j}\frac{2Z_4}{\pi k_2 R_4\left[\mathrm{J}_1(k_2R_4)\mathrm{Y}_1(k_2R_3)-\mathrm{J}_1(k_2R_3)\mathrm{Y}_1(k_2R_4)\right]},
\tag{6}
$$

$$
\begin{aligned}
Z_{\mathrm{m31}} &= \mathrm{j}\frac{2Z_5}{\pi k_3 R_5\left[\mathrm{J}_1(k_3R_6)\mathrm{Y}_1(k_3R_5)-\mathrm{J}_1(k_3R_5)\mathrm{Y}_1(k_3R_6)\right]}\\
&\quad\times\left[\frac{\mathrm{J}_1(k_3R_6)\mathrm{Y}_0(k_3R_5)-\mathrm{J}_0(k_3R_5)\mathrm{Y}_1(k_3R_6)-\mathrm{J}_1(k_3R_5)\mathrm{Y}_0(k_3R_5)+\mathrm{J}_0(k_3R_5)\mathrm{Y}_1(k_3R_5)}{\mathrm{J}_1(k_3R_5)\mathrm{Y}_0(k_3R_5)-\mathrm{J}_0(k_3R_5)\mathrm{Y}_1(k_3R_5)}\right]\\
&\quad-\mathrm{j}\frac{2Z_5(1-\sigma 3)}{\pi(k_3R_5)^2\left[\mathrm{J}_1(k_3R_5)\mathrm{Y}_0(k_3R_5)-\mathrm{J}_0(k_3R_5)\mathrm{Y}_1(k_3R_5)\right]},
\end{aligned}
\tag{7}
$$

$$
\begin{aligned}
Z_{\mathrm{m32}} &= \mathrm{j}\frac{2Z_5}{\pi k_3 R_5\left[\mathrm{J}_1(k_3R_6)\mathrm{Y}_1(k_3R_5)-\mathrm{J}_1(k_3R_5)\mathrm{Y}_1(k_3R_6)\right]}\\
&\quad\times\left[\frac{\mathrm{J}_1(k_3R_5)\mathrm{Y}_0(k_3R_6)-\mathrm{J}_0(k_3R_6)\mathrm{Y}_1(k_3R_5)-\mathrm{J}_1(k_3R_6)\mathrm{Y}_0(k_3R_6)+\mathrm{J}_0(k_3R_6)\mathrm{Y}_1(k_3R_6)}{\mathrm{J}_1(k_3R_6)\mathrm{Y}_0(k_3R_6)-\mathrm{J}_0(k_3R_6)\mathrm{Y}_1(k_3R_6)}\right]\\
&\quad+\mathrm{j}\frac{2Z_6(1-\sigma 3)}{\pi(k_3R_6)^2\left[\mathrm{J}_1(k_3R_6)\mathrm{Y}_0(k_3R_6)-\mathrm{J}_0(k_3R_6)\mathrm{Y}_1(k_3R_6)\right]},
\end{aligned}
\tag{8}
$$

$$
Z_{\mathrm{m33}} = \mathrm{j}\frac{2Z_5}{\pi k_3 R_5\left[\mathrm{J}_1(k_3R_6)\mathrm{Y}_1(k_3R_5)-\mathrm{J}_1(k_3R_5)\mathrm{Y}_1(k_3R_6)\right]} = \mathrm{j}\frac{2Z_6}{\pi k_3 R_6\left[\mathrm{J}_1(k_3R_6)\mathrm{Y}_1(k_3R_5)-\mathrm{J}_1(k_3R_5)\mathrm{Y}_1(k_3R_6)\right]},
\tag{9}
$$

where $\mathrm{J}_0(k_ir)$ and $\mathrm{Y}_0(k_ir)$ are the Bessel functions of the first and second kinds of order zero, respectively; $\mathrm{J}_1(k_ir)$ and $\mathrm{Y}_1(k_ir)$ are the Bessel functions of the first and second kinds of order one, respectively; and $i=1,2,3$. Imaginary unit $\mathrm{j}=\sqrt{-1}$; $Z_1=\rho_1 c_{\mathrm{m1}}S_1$, $Z_2=\rho_1 c_{\mathrm{m1}}S_2$, $Z_3=\rho_2 c_{\mathrm{m2}}S_3$, $Z_4=\rho_2 c_{\mathrm{m2}}S_4$, $Z_5=\rho_3 c_{\mathrm{m3}}S_5$, $Z_6=\rho_3 c_{\mathrm{m3}}S_6$, $S_1=2\pi R_1 h$, $S_2=2\pi R_2 h$, $S_3=2\pi R_3 h$, $S_4=2\pi R_4 h$, $S_5=2\pi R_5 h$, $S_6=2\pi R_6 h$; $k_i=\omega/c_{\mathrm{m}i}$ is the wave number of radial vibration; $c_{\mathrm{m}i}=\sqrt{E_i/\left(\rho_i\left(1-\sigma_i^2\right)\right)}$ is the sound speed of radial vibration; $\omega=2\pi f$ is angular frequency, f is the frequency. E_i, ρ_i, σ_i are Young's modulus, density and Poisson's ratio of short metal tube. Z_{p11}, Z_{p12}, Z_{p13}, Z_{p21}, Z_{p22} and Z_{p23} are the mechanical impedances of the piezoceramics short tubes. V_1 and V_2 are the input excitation voltages and $V_1=V_2$; C_{or1}, C_{or2} and N_1, N_2 are the clamping capacitances and electromechanical conversion coefficients. Their expressions are as follows:[18]

$$
\begin{aligned}
Z_{\mathrm{p11}} &= -Z_{01}\frac{\mathrm{j}R_3^2M_3^2\left[\mathrm{J}_\upsilon(k_{\mathrm{r}1}R_3)\mathrm{Y}_{\upsilon-1}(k_{\mathrm{r}1}R_2)-\mathrm{J}_{\upsilon-1}(k_{\mathrm{r}1}R_2)\mathrm{Y}_\upsilon(k_{\mathrm{r}1}R_3)\right]}{\mathrm{J}_\upsilon(k_{\mathrm{r}1}R_2)\mathrm{Y}_\upsilon(k_{\mathrm{r}1}R_3)-\mathrm{J}_\upsilon(k_{\mathrm{r}1}R_3)\mathrm{Y}_\upsilon(k_{\mathrm{r}1}R_2)}\\
&\quad+\frac{\mathrm{j}2\pi hR_3^2M_3^2(c_2-c_3\upsilon)}{\omega}+Z_{01}\frac{\mathrm{j}2R_3M_2M_3}{\pi k_{\mathrm{r}1}\left[\mathrm{J}_\upsilon(k_{\mathrm{r}1}R_2)\mathrm{Y}_\upsilon(k_{\mathrm{r}1}R_3)-\mathrm{J}_\upsilon(k_{\mathrm{r}1}R_3)\mathrm{Y}_\upsilon(k_{\mathrm{r}1}R_2)\right]},
\end{aligned}
\tag{10}
$$

$$
\begin{aligned}
Z_{\mathrm{p12}} &= -Z_{02}\frac{\mathrm{j}R_2^2M_2^2\left[\mathrm{J}_\upsilon(k_{\mathrm{r}1}R_2)\mathrm{Y}_{\upsilon-1}(k_{\mathrm{r}1}R_3)-\mathrm{J}_{\upsilon-1}(k_{\mathrm{r}1}R_3)\mathrm{Y}_\upsilon(k_{\mathrm{r}1}R_2)\right]}{\mathrm{J}_\upsilon(k_{\mathrm{r}1}R_2)\mathrm{Y}_\upsilon(k_{\mathrm{r}1}R_3)-\mathrm{J}_\upsilon(k_{\mathrm{r}1}R_3)\mathrm{Y}_\upsilon(k_{\mathrm{r}1}R_2)}\\
&\quad+\frac{\mathrm{j}2\pi hR_2^2M_2^2(c_3\upsilon-c_2)}{\omega}+Z_{02}\frac{\mathrm{j}2R_2M_2M_3}{\pi k_{\mathrm{r}1}\left[\mathrm{J}_\upsilon(k_{\mathrm{r}1}R_2)\mathrm{Y}_\upsilon(k_{\mathrm{r}1}R_3)-\mathrm{J}_\upsilon(k_{\mathrm{r}1}R_3)\mathrm{Y}_\upsilon(k_{\mathrm{r}1}R_2)\right]},
\end{aligned}
\tag{11}
$$

$$
\begin{aligned}
Z_{\mathrm{p13}} &= -Z_{01}\frac{\mathrm{j}2R_3M_2M_3}{\pi k_{\mathrm{r}1}\left[\mathrm{J}_\upsilon(k_{\mathrm{r}1}R_2)\mathrm{Y}_\upsilon(k_{\mathrm{r}1}R_3)-\mathrm{J}_\upsilon(k_{\mathrm{r}1}R_3)\mathrm{Y}_\upsilon(k_{\mathrm{r}1}R_2)\right]}\\
&= -Z_{02}\frac{\mathrm{j}2R_2M_2M_3}{\pi k_{\mathrm{r}1}\left[\mathrm{J}_\upsilon(k_{\mathrm{r}1}R_2)\mathrm{Y}_\upsilon(k_{\mathrm{r}1}R_3)-\mathrm{J}_\upsilon(k_{\mathrm{r}1}R_3)\mathrm{Y}_\upsilon(k_{\mathrm{r}1}R_2)\right]},
\end{aligned}
\tag{12}
$$

$$Z_{\mathrm{p21}} = -Z_{03}\frac{\mathrm{j}R_5^2M_5^2\left[\mathrm{J}_\upsilon(k_{\mathrm{r}2}R_5)\mathrm{Y}_{\upsilon-1}(k_{\mathrm{r}2}R_4)-\mathrm{J}_{\upsilon-1}(k_{\mathrm{r}2}R_4)\mathrm{Y}_\upsilon(k_{\mathrm{r}2}R_5)\right]}{\mathrm{J}_\upsilon(k_{\mathrm{r}2}R_4)\mathrm{Y}_\upsilon(k_{\mathrm{r}2}R_5)-\mathrm{J}_\upsilon(k_{\mathrm{r}2}R_5)\mathrm{Y}_\upsilon(k_{\mathrm{r}2}R_4)} + \frac{\mathrm{j}2\pi hR_5^2M_5^2(c_2-c_3\upsilon)}{\omega} + Z_{03}\frac{\mathrm{j}2R_5M_4M_5}{\pi k_{\mathrm{r}2}\left[\mathrm{J}_\upsilon(k_{\mathrm{r}2}R_4)\mathrm{Y}_\upsilon(k_{\mathrm{r}2}R_5)-\mathrm{J}_\upsilon(k_{\mathrm{r}2}R_5)\mathrm{Y}_\upsilon(k_{\mathrm{r}2}R_4)\right]}, \tag{13}$$

$$Z_{\mathrm{p22}} = -Z_{04}\frac{\mathrm{j}R_4^2M_4^2\left[\mathrm{J}_\upsilon(k_{\mathrm{r}2}R_4)\mathrm{Y}_{\upsilon-1}(k_{\mathrm{r}2}R_5)-\mathrm{J}_{\upsilon-1}(k_{\mathrm{r}2}R_5)\mathrm{Y}_\upsilon(k_{\mathrm{r}2}R_4)\right]}{\mathrm{J}_\upsilon(k_{\mathrm{r}2}R_4)\mathrm{Y}_\upsilon(k_{\mathrm{r}2}R_5)-\mathrm{J}_\upsilon(k_{\mathrm{r}2}R_5)\mathrm{Y}_\upsilon(k_{\mathrm{r}2}R_4)} + \frac{\mathrm{j}2\pi hR_4^2M_4^2(c_3\upsilon-c_2)}{\omega} + Z_{04}\frac{\mathrm{j}2R_4M_4M_5}{\pi k_{\mathrm{r}2}\left[\mathrm{J}_\upsilon(k_{\mathrm{r}2}R_4)\mathrm{Y}_\upsilon(k_{\mathrm{r}2}R_5)-\mathrm{J}_\upsilon(k_{\mathrm{r}2}R_5)\mathrm{Y}_\upsilon(k_{\mathrm{r}2}R_4)\right]}, \tag{14}$$

$$Z_{\mathrm{p23}} = -Z_{03}\frac{\mathrm{j}2R_5M_4M_5}{\pi k_{\mathrm{r}2}\left[\mathrm{J}_\upsilon(k_{\mathrm{r}2}R_4)\mathrm{Y}_\upsilon(k_{\mathrm{r}2}R_5)-\mathrm{J}_\upsilon(k_{\mathrm{r}2}R_5)\mathrm{Y}_\upsilon(k_{\mathrm{r}2}R_4)\right]} = -Z_{04}\frac{\mathrm{j}2R_4M_4M_5}{\pi k_{\mathrm{r}2}\left[\mathrm{J}_\upsilon(k_{\mathrm{r}2}R_4)\mathrm{Y}_\upsilon(k_{\mathrm{r}2}R_5)-\mathrm{J}_\upsilon(k_{\mathrm{r}2}R_5)\mathrm{Y}_\upsilon(k_{\mathrm{r}2}R_4)\right]}, \tag{15}$$

$$C_{\mathrm{or1}} = 2\pi ht, \quad C_{\mathrm{or2}} = 2\pi ht_0, \tag{16}$$

$$N_1 = 2\pi htk_{\mathrm{r}1}R_2R_3M_2M_3, \quad N_2 = 2\pi ht_0k_{\mathrm{r}2}R_4R_5M_4M_5. \tag{17}$$

Here, $\mathrm{J}_\upsilon\left(k_{\mathrm{r}\gamma}r\right)$ and $\mathrm{Y}_\upsilon\left(k_{\mathrm{r}\gamma}r\right)$ are the Bessel functions of the first and second kinds of order υ, respectively; $\mathrm{J}_{\upsilon-1}\left(k_{\mathrm{r}\gamma}r\right)$ and $\mathrm{Y}_{\upsilon-1}\left(k_{\mathrm{r}\gamma}r\right)$ are the Bessel functions of the first and second kinds of order $\upsilon-1$, respectively; and $\gamma=1,2$. $Z_{01}=\rho_{\mathrm{r}1}c_{\mathrm{r}1}S_2$, $Z_{02}=\rho_{\mathrm{r}1}c_{\mathrm{r}1}S_3$, $Z_{03}=\rho_{\mathrm{r}2}c_{\mathrm{r}2}S_4$, $Z_{04}=\rho_{\mathrm{r}2}c_{\mathrm{r}2}S_5$; $k_{\mathrm{r}\gamma}=\omega/c_{\mathrm{r}\gamma}$ is the wave number of radial vibration; $c_{\mathrm{r}\gamma}=\sqrt{c_3/\rho_{\mathrm{r}\gamma}}$ is the sound speed of radial vibration; $\rho_{\mathrm{r}\gamma}$ is the density of the piezoelectric ceramic short tube; $c_{\alpha\beta}^{\mathrm{E}}$, $e_{\alpha\beta}$, $\varepsilon_{\alpha\beta}^{\mathrm{S}}$ are elastic constants, piezoelectric constants and dielectric constants, respectively; $n_1=R_3M_3$, $n_2=R_2M_2$, $n_3=R_5M_5$, $n_4=R_4M_4$. The specific expressions of M_2, M_3, M_4, M_5, c_1, c_2, c_3, υ, t, t_0 in Eqs. (10)–(17) are listed in Appendix A.

By performing a series of circuit transformations on the electromechanical equivalent circuit of Fig. 2, a simplified equivalent circuit is obtained, as shown in Fig. 3.

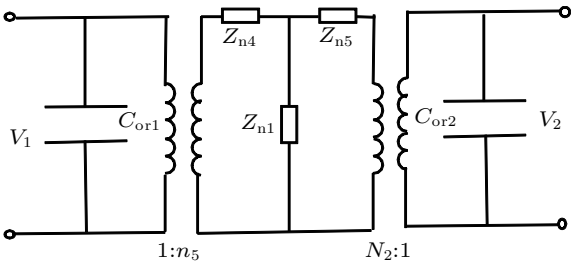


Fig. 3. Simplified equivalent circuit.

In Fig. 3, the specific expressions of impedances are as follows:

$$Z_{\mathrm{n4}} = Z_{\mathrm{b1}} + Z_{\mathrm{n3}}, \tag{18}$$

$$Z_{\mathrm{n5}} = Z_{\mathrm{n2}} + Z_{\mathrm{a3}}, \tag{19}$$

$$Z_{\mathrm{n1}} = \frac{Z_{\mathrm{d1}}Z_{\mathrm{d2}}}{Z_{\mathrm{d1}}+Z_{\mathrm{d2}}+Z_{\mathrm{c3}}}, \tag{20}$$

$$Z_{\mathrm{n2}} = \frac{Z_{\mathrm{c3}}Z_{\mathrm{d2}}}{Z_{\mathrm{d1}}+Z_{\mathrm{d2}}+Z_{\mathrm{c3}}}, \tag{21}$$

$$Z_{\mathrm{n3}} = \frac{Z_{\mathrm{c3}}Z_{\mathrm{d1}}}{Z_{\mathrm{d1}}+Z_{\mathrm{d2}}+Z_{\mathrm{c3}}}, \tag{22}$$

$$Z_{\mathrm{d1}} = \frac{Z_{\mathrm{b3}}Z_{\mathrm{c1}}}{Z_{\mathrm{b3}}+Z_{\mathrm{c1}}}, \tag{23}$$

$$Z_{\mathrm{d2}} = \frac{Z_{\mathrm{c4}}Z_{\mathrm{a4}}}{Z_{\mathrm{c4}}+Z_{\mathrm{a4}}}, \tag{24}$$

$$Z_{\mathrm{c1}} = Z_{\mathrm{b2}} + Z_{\mathrm{b4}} + \frac{Z_{\mathrm{b2}}Z_{\mathrm{b4}}}{Z_{\mathrm{b5}}}, \tag{25}$$

$$Z_{\mathrm{c2}} = Z_{\mathrm{b4}} + Z_{\mathrm{b5}} + \frac{Z_{\mathrm{b4}}Z_{\mathrm{b5}}}{Z_{\mathrm{b2}}}, \tag{26}$$

$$Z_{\mathrm{c3}} = Z_{\mathrm{b2}} + Z_{\mathrm{b5}} + \frac{Z_{\mathrm{b2}}Z_{\mathrm{b5}}}{Z_{\mathrm{b4}}}, \tag{27}$$

$$Z_{\mathrm{b1}} = \frac{Z_{\mathrm{a1}}n_3^2}{n_2^2}, \tag{28}$$

$$Z_{\mathrm{b2}} = \frac{Z_{\mathrm{p12}}n_3^2}{n_2^2}Z_{\mathrm{p22}} + n_3^2Z_{\mathrm{m21}}, \tag{29}$$

$$Z_{\mathrm{b3}} = \frac{Z_{\mathrm{a2}}n_3^2}{n_2^2}, \tag{30}$$

$$Z_{\mathrm{b4}} = n_3^2Z_{\mathrm{m23}}, \tag{31}$$

$$Z_{\mathrm{b5}} = Z_{\mathrm{p21}} + n_3^2Z_{\mathrm{m22}}, \tag{32}$$

$$n_5 = \frac{n_3N_1}{n_2}, \tag{33}$$

$$Z_{\mathrm{a1}} = Z_{\mathrm{p13}} - \frac{N_1^2}{\mathrm{j}\omega C_{\mathrm{or1}}}, \tag{34}$$

$$Z_{\mathrm{a2}} = Z_{\mathrm{p11}} + n_1^2Z_{\mathrm{m}i}, \tag{35}$$

$$Z_{\mathrm{a3}} = Z_{\mathrm{p23}} - \frac{N_2^2}{\mathrm{j}\omega C_{\mathrm{or2}}}, \tag{36}$$

$$Z_{\mathrm{a4}} = Z_{\mathrm{p22}} + n_4^2Z_{\mathrm{mo}}, \tag{37}$$

$$Z_{\mathrm{m}i} = Z_{\mathrm{m12}} + \frac{(Z_{\mathrm{m11}}+Z_{l1})Z_{\mathrm{m13}}}{(Z_{\mathrm{m11}}+Z_{l1})+Z_{\mathrm{m13}}}, \quad Z_{\mathrm{mo}} = Z_{\mathrm{m31}} + \frac{(Z_{\mathrm{m32}}+Z_{l2})Z_{\mathrm{m33}}}{(Z_{\mathrm{m32}}+Z_{l2})+Z_{\mathrm{m33}}}, \tag{38}$$

where the total mechanical resistances of short metal tubes (m_1, m_3) are defined as $Z_{\mathrm{m}i}$ and Z_{mo}, respectively. Under no-load condition, $Z_{l1}=Z_{l2}=0$. The expression of the input electrical impedance of radial cascaded composite ultrasonic

transducer can be obtained from Fig. 3, as shown in the following form:

$$Z_{\mathrm{e}} = \frac{Z_{\mathrm{e1}} Z_{\mathrm{e2}}}{Z_{\mathrm{e1}} + Z_{\mathrm{e2}}}. \tag{39}$$

Here, the input electrical impedances of the piezoelectric ceramic short tube (p_1, p_2) are Z_{e1} and Z_{e2}, whose expressions are as follows:

$$Z_{\mathrm{e1}} = \frac{Z_{\mathrm{mr1}}}{\mathrm{j}\omega Z_{\mathrm{mr1}} C_{\mathrm{or1}} + n_5^2}, \tag{40}$$

$$Z_{\mathrm{e2}} = \frac{Z_{\mathrm{mr2}}}{\mathrm{j}\omega Z_{\mathrm{mr2}} C_{\mathrm{or2}} + N_2^2}, \tag{41}$$

$$Z_{\mathrm{mr1}} = \frac{(Z_{\mathrm{n1}} + Z_{\mathrm{n5}})(Z_{\mathrm{n1}} + Z_{\mathrm{n4}}) - Z_{\mathrm{n1}}^2}{(Z_{\mathrm{n1}} + Z_{\mathrm{n5}}) - N_2/n_5 Z_{\mathrm{n1}}}, \tag{42}$$

$$Z_{\mathrm{mr2}} = \frac{(Z_{\mathrm{n1}} + Z_{\mathrm{n5}})(Z_{\mathrm{n1}} + Z_{\mathrm{n4}}) - Z_{\mathrm{n1}}^2}{(Z_{\mathrm{n1}} + Z_{\mathrm{n4}}) - n_5/N_2 Z_{\mathrm{n1}}}. \tag{43}$$

The resonance frequency equation, anti-resonance frequency equation and the expression of the effective electromechanical coupling coefficient of the radial cascaded composite ultrasonic transducer are as follows:

$$Z_{\mathrm{e}} = \frac{Z_{\mathrm{e1}} Z_{\mathrm{e2}}}{Z_{\mathrm{e1}} + Z_{\mathrm{e2}}} = 0, \tag{44}$$

$$Z_{\mathrm{e}} = \frac{Z_{\mathrm{e1}} Z_{\mathrm{e2}}}{Z_{\mathrm{e1}} + Z_{\mathrm{e2}}} \to \infty, \tag{45}$$

$$K_{\mathrm{eff}} = \sqrt{1 - f_{\mathrm{r}}^2 / f_{\mathrm{a}}^2}, \tag{46}$$

where f_{r} and f_{a} are the resonance frequency and anti-resonance frequency of the radial vibration of the transducer. From Eqs. (44)–(46), when the geometric dimensions and material parameters of the transducer are given, the resonance/anti-resonance frequency can be determined, and then the effective electromechanical coupling coefficient can be obtained. Different resonance/antiresonance frequencies correspond to different vibrational modes. Each resonance/anti-resonance frequency corresponds to an effective electromechanical coupling coefficient.

3. Analysis of vibration characteristics of radial cascaded composite ultrasonic transducer

In order to optimize the electromechanical characteristics of radial vibration of the transducers, the theoretical relationships between the radial dimensions of piezoelectric short tubes and the resonance (f_{r})/anti-resonance (f_{a}) frequencies and the effective electromechanical coupling coefficients (K_{eff}) are studied in this section. Because Eqs. (44)–(46) are transcendental equations, Wolfram Mathematica 8.0 is used to solve analytical theory. Herein, the short metal tubes (m_1, m_2, and m_3) are selected as steel, aluminum and aluminum, and the piezoelectric ceramic short tubes (p_1, p_2) are all selected as PZT-4. The standard parameters of these materials are as follows: $E_1 = 2.05 \times 10^{11}$ N/m^2, $\rho_1 = 7850$ kg/m^3, $\sigma_1 = 0.28$; $E_2 = E_3 = 7 \times 10^{10}$ N/m^2, $\rho_2 = \rho_3 = 2700$ kg/m^3, $\sigma_2 = \sigma_3 = 0.33$; $\rho_{\mathrm{r}\gamma} = 7500$ kg/m^3, $c_{11}^{\mathrm{E}} = 13.9 \times 10^{10}$ N·m^{-2}, $c_{12}^{\mathrm{E}} = 7.78 \times 10^{10}$ N·m^{-2}, $c_{13}^{\mathrm{E}} = 7.43 \times 10^{10}$ N·m^{-2}, $c_{33}^{\mathrm{E}} = 11.5 \times 10^{10}$ N·m^{-2}, $e_{31} = -5.2$ C·m^{-2}, $e_{33} = 15.1$ C·m^{-2}, $\varepsilon_{33}^{\mathrm{S}}/\varepsilon_0$=635, $\varepsilon_0 = 8.854 \times 10^{-12}$ F·m^{-1}.

The theoretical relationships between the radial dimensions of the piezoelectric ceramic short tube p_1 and the resonance/anti-resonance frequencies, the effective electromechanical coupling coefficients are analyzed, as shown in Figs. 4 and 5. In the calculation, R_2 is gradually changed and other geometric dimensions are fixed ($R_1 = 11$ mm, $R_3 = 19$ mm, $R_4 = 23$ mm, $R_5 = 27$ mm, $R_6 = 31$ mm and $h = 5$ mm). As can be seen from Figs. 4 and 5, as R_2 increases, the first-order resonance (f_{r1})/antiresonance (f_{a1}) frequencies both increase while the effective electromechanical coupling coefficient (K_{eff1}) decreases. When R_2 is at certain values, both the second-order anti-resonance frequency (f_{a2}) and the effective electromechanical coupling coefficient (K_{eff2}) of the transducer have maximum values, which is crucial to the engineering design and application of the transducer.

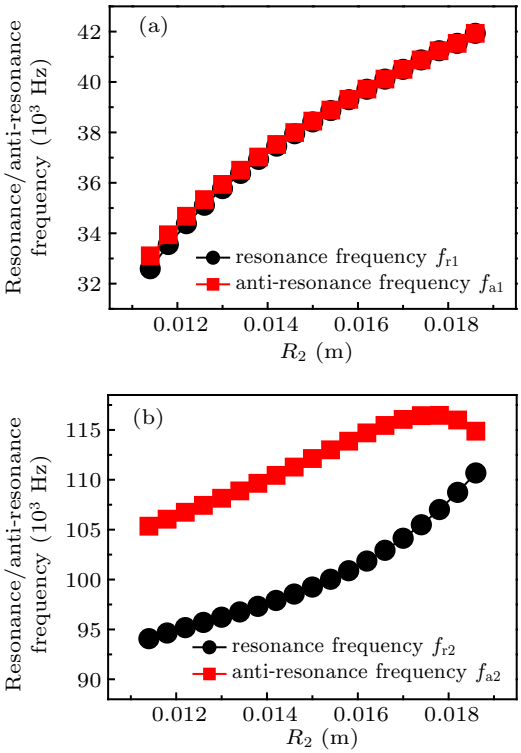


Fig. 4. Theoretical relationships between the radial dimensions of p_1 and the resonance/anti-resonance frequencies: (a) the fundamental mode, (b) the second mode.

The theoretical relationships between the radial dimensions of the piezoelectric ceramic short tube p_2 and the resonance/antiresonance frequencies, the effective electromechanical coupling coefficients are analyzed, as shown in Figs. 6 and 7. In the calculation, R_4 gradually changed and other geometric dimensions are fixed ($R_1 = 11$ mm, $R_2 = 15$ mm,

$R_3 = 19$ mm, $R_5 = 27$ mm, $R_6 = 31$ mm and $h = 5$ mm). As can be seen from Figs. 6 and 7, as R_4 increases, the first-order resonance (f_{r1})/anti-resonance (f_{a1}) frequencies increase, and the effective electromechanical coupling coefficient (K_{eff1}) responding to the fundamental mode has a maximum value. When R_4 is at a certain value, the second-order anti-resonance frequency (f_{a2}) has a minimum value, which should be avoided in the actual design of the transducer.

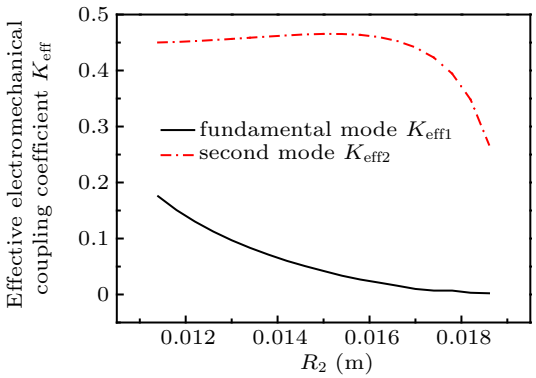


Fig. 5. Theoretical relationships between the radial dimensions of p_1 and the effective electromechanical coupling coefficients.

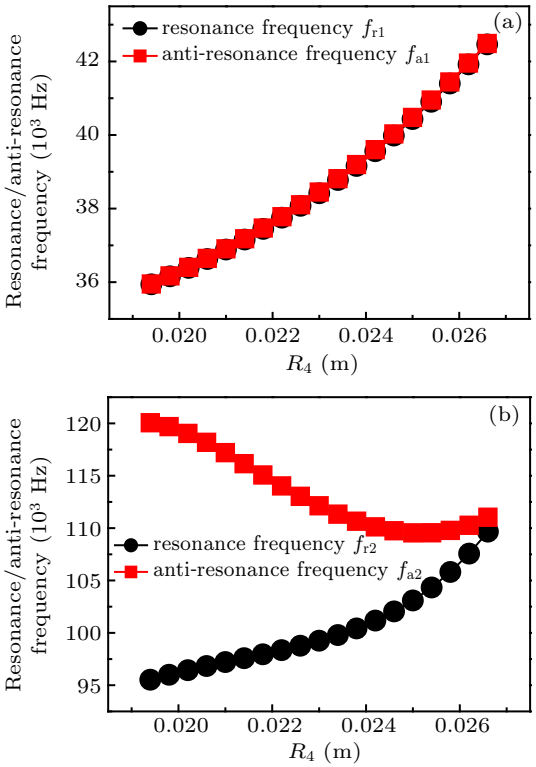


Fig. 6. Theoretical relationships between the radial dimensions of p_2 and the resonance/anti-resonance frequencies: (a) the fundamental mode, (b) the second mode.

It can be clearly seen from Figs. 4–7 that the resonance/anti-resonance frequency and effective electromechanical coupling coefficient of the transducer are all related to the radial dimensions of the piezoelectric ceramic short tube. Under the same conditions, the effective electromechanical coupling coefficients of the transducer at the second mode are much larger than those at the fundamental mode (Figs. 5 and 7). Therefore, the radial cascaded composite ultrasonic transducer should be worked at the second mode to ensure a higher electromechanical conversion capability. The conclusions of this section have certain reference value for the engineering design and application of transducer.

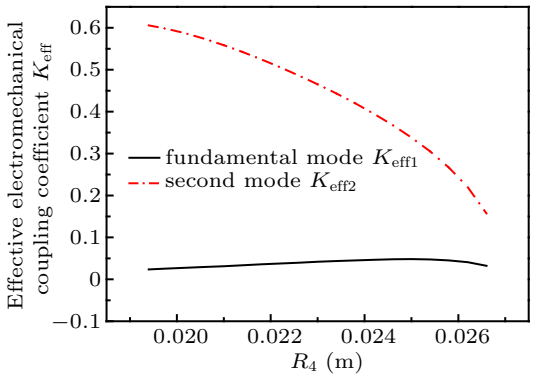


Fig. 7. Theoretical relationships between the radial dimensions of p_2 and the effective electromechanical coupling coefficient.

4. Experiments

In this section, the experiments are carried out to verify the correctness of the analytical theory. Based on the conclusions in Section 3, two prototypes of radial cascaded composite ultrasonic transducer are designed and manufactured, whose geometric dimensions are listed in Table 1. The piezoelectric and metallic materials of the transducer are consistent with those in Section 3.

Table 1. Geometric dimensions of two radial cascaded composite ultrasonic transducers.

No.	R_1 (m)	R_2 (m)	R_3 (m)	R_4 (m)	R_5 (m)	R_6 (m)	h (m)
1	0.014	0.018	0.021	0.025	0.028	0.032	0.006
2	0.016	0.019	0.022	0.026	0.030	0.033	0.005

For comparison, the first-order and second-order resonance/anti-resonance frequencies of the transducers are displayed in Tables 2 and 3. Herein, theoretical results are calculated by Eqs. (44) and (45). The numerical results are obtained by COMSOL Multiphysics 5.4, and the vibrational modes of transducer 1 at the fundamental mode and the second mode are shown in Fig. 8. The experimental results are measured by a WK6500B precision impedance analyzer. The experimental device is displayed in Fig. 9, and the magnitude and phase of the input electric impedance of transducer 1 are measured, as shown in Fig. 10.

Table 2. Resonance frequencies and anti-resonance frequencies of the transducers at the fundamental mode.

No.	Theoretical results		Numerical results		Experimental results	
	f_r/Hz	f_a/Hz	f_{rn}/Hz	f_{an}/Hz	f_{rm}/Hz	f_{am}/Hz
1	34909	35040	34928	35058	34242	34546
2	30573	30820	30622	30847	30202	30414

Table 3. Resonance frequencies and anti-resonance frequencies of the transducers at the second mode.

No.	Theoretical results		Numerical results		Experimental results	
	f_r/Hz	f_a/Hz	f_{rn}/Hz	f_{an}/Hz	f_{rm}/Hz	f_{am}/Hz
1	108722	122096	113120	124950	105758	109798
2	108169	123248	113230	125380	104416	108368

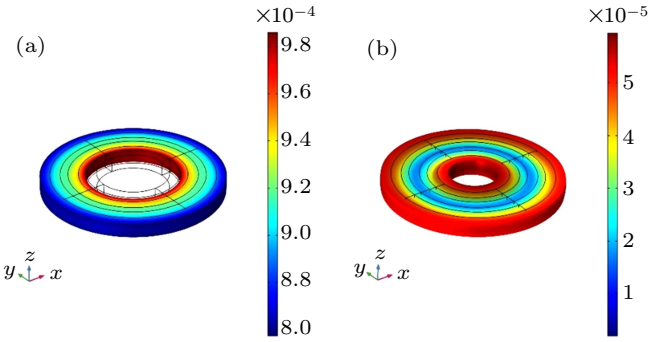


Fig. 8. Vibrational modes of transducer 1: (a) the fundamental mode, (b) the second mode.

In Tables 2 and 3, f_r, f_a, f_{rn}, f_{an} and f_{rm}, f_{am} are the theoretical, numerical and experimental resonance frequencies and anti-resonance frequencies, respectively. Obviously, when the transducers are vibrating at the fundamental mode and the second mode, the theoretical results are consistent with the numerical results and the experimental results. For the frequency errors, the main reasons are as follows: (1) In the experiments, the coupling between modes affects the vibration of the transducer, which is inconsistent with the theoretical analysis. (2) The standard material parameters of the theoretical analysis are not exactly the same as the actual material parameters. (3) The losses and loads are ignored in the theoretical analysis. (4) The complexity of the actual fabrication of the transducer, such as the incomplete application of conductive glue, has a certain impact on the experimental results.



Fig. 9. Experimental device for measuring frequency characteristics of the transducers.

(a) resonance frequency = 34242 Hz

(b) resonance frequency = 105758 Hz

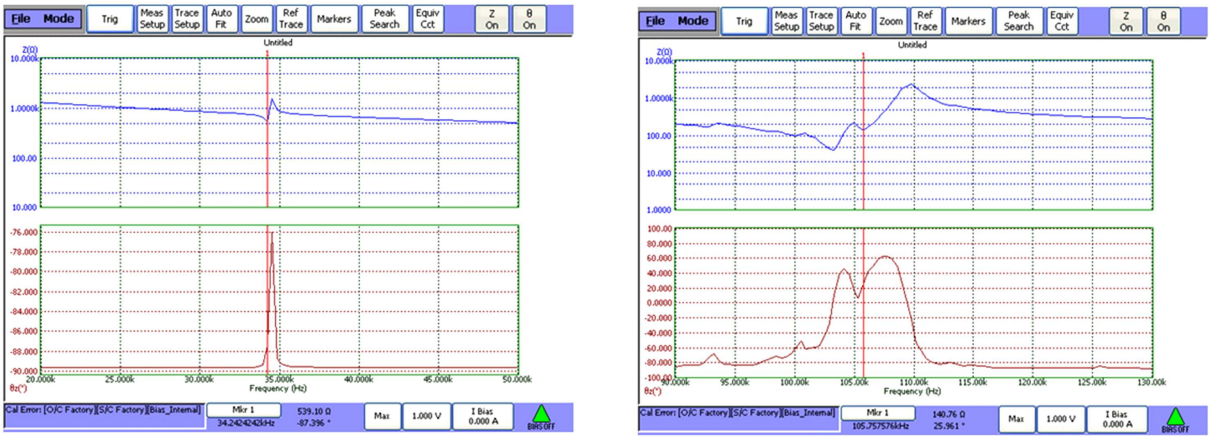


Fig. 10. Magnitude and phase of the input electric impedance of transducer 1: (a) the fundamental mode, (b) the second mode.

5. Conclusions

The radial vibration of radial cascaded composite ultrasonic transducer is analyzed. Based on the plane stress theory, the electromechanical equivalent circuit of the transducer is derived for the first time. The theoretical relationships between the electromechanical characteristics and the radial dimension are studied. Analyzing the study results, we can draw the following conclusions:

(1) The theoretical resonance/anti-resonance frequencies are consistent with the numerical and experimental results.

(2) The other geometric dimensions of the transducer are fixed, when R_2 is at certain values, the anti-resonance frequency and effective electromechanical coupling coefficient responding to the second mode have maximum values. When R_4 at a certain value, the second-order anti-resonance frequency has a minimum value.

(3) Under the same conditions, the effective electromechanical coupling coefficients at the second mode are much larger than those at the fundamental mode.

Appendix A

The specific expressions of M_2, M_3, M_4, M_5, c_1, c_2, c_3, υ, t, t_0 in Eqs. (10)–(17) are listed as follows:

$$
\begin{aligned}
M_2 &= F_1\left\{(\upsilon-2)s_{-2,\upsilon-1}(k_{\mathrm{r}1}R_2)-\frac{[\mathrm{J}_{\upsilon-1}(k_{\mathrm{r}1}R_2)\mathrm{Y}_\upsilon(k_{\mathrm{r}1}R_3)-\mathrm{J}_\upsilon(k_{\mathrm{r}1}R_3)\mathrm{Y}_{\upsilon-1}(k_{\mathrm{r}1}R_2)]\,s_{-1,\upsilon}(k_{\mathrm{r}1}R_2)}{\mathrm{J}_\upsilon(k_{\mathrm{r}1}R_2)\mathrm{Y}_\upsilon(k_{\mathrm{r}1}R_3)-\mathrm{J}_\upsilon(k_{\mathrm{r}1}R_3)\mathrm{Y}_\upsilon(k_{\mathrm{r}1}R_2)}\right.\\
&\quad\left.-\frac{2s_{-1,\upsilon}(k_{\mathrm{r}1}R_3)}{\pi k_{\mathrm{r}1}R_2\,[\mathrm{J}_\upsilon(k_{\mathrm{r}1}R_2)\mathrm{Y}_\upsilon(k_{\mathrm{r}1}R_3)-\mathrm{J}_\upsilon(k_{\mathrm{r}1}R_3)\mathrm{Y}_\upsilon(k_{\mathrm{r}1}R_2)]}\right\}+\frac{F_2}{k_{\mathrm{r}1}R_2},\\
M_3 &= F_1\left\{(\upsilon-2)s_{-2,\upsilon-1}(k_{\mathrm{r}1}R_3)-\frac{[\mathrm{J}_{\upsilon-1}(k_{\mathrm{r}1}R_3)\mathrm{Y}_\upsilon(k_{\mathrm{r}1}R_2)-\mathrm{J}_\upsilon(k_{\mathrm{r}1}R_2)\mathrm{Y}_{\upsilon-1}(k_{\mathrm{r}1}R_3)]\,s_{-1,\upsilon}(k_{\mathrm{r}1}R_3)}{\mathrm{J}_\upsilon(k_{\mathrm{r}1}R_2)\mathrm{Y}_\upsilon(k_{\mathrm{r}1}R_3)-\mathrm{J}_\upsilon(k_{\mathrm{r}1}R_3)\mathrm{Y}_\upsilon(k_{\mathrm{r}1}R_2)}\right.\\
&\quad\left.+\frac{2s_{-1,\upsilon}(k_{\mathrm{r}1}R_2)}{\pi k_{\mathrm{r}1}R_3\,[\mathrm{J}_\upsilon(k_{\mathrm{r}1}R_2)\mathrm{Y}_\upsilon(k_{\mathrm{r}1}R_3)-\mathrm{J}_\upsilon(k_{\mathrm{r}1}R_3)\mathrm{Y}_\upsilon(k_{\mathrm{r}1}R_2)]}\right\}+\frac{F_2}{k_{\mathrm{r}1}R_3},\\
M_4 &= F_1\left\{(\upsilon-2)s_{-2,\upsilon-1}(k_{\mathrm{r}2}R_4)-\frac{[\mathrm{J}_{\upsilon-1}(k_{\mathrm{r}2}R_4)\mathrm{Y}_\upsilon(k_{\mathrm{r}2}R_5)-\mathrm{J}_\upsilon(k_{\mathrm{r}2}R_5)\mathrm{Y}_{\upsilon-1}(k_{\mathrm{r}2}R_4)]\,s_{-1,\upsilon}(k_{\mathrm{r}2}R_4)}{\mathrm{J}_\upsilon(k_{\mathrm{r}2}R_4)\mathrm{Y}_\upsilon(k_{\mathrm{r}2}R_5)-\mathrm{J}_\upsilon(k_{\mathrm{r}2}R_5)\mathrm{Y}_\upsilon(k_{\mathrm{r}2}R_4)}\right.\\
&\quad\left.-\frac{2s_{-1,\upsilon}(k_{\mathrm{r}2}R_5)}{\pi k_{\mathrm{r}2}R_4\,[\mathrm{J}_\upsilon(k_{\mathrm{r}2}R_4)\mathrm{Y}_\upsilon(k_{\mathrm{r}2}R_5)-\mathrm{J}_\upsilon(k_{\mathrm{r}2}R_5)\mathrm{Y}_\upsilon(k_{\mathrm{r}2}R_4)]}\right\}+\frac{F_2}{k_{\mathrm{r}2}R_4},\\
M_5 &= F_1\left\{(\upsilon-2)s_{-2,\upsilon-1}(k_{\mathrm{r}2}R_5)-\frac{[\mathrm{J}_{\upsilon-1}(k_{\mathrm{r}2}R_5)\mathrm{Y}_\upsilon(k_{\mathrm{r}2}R_4)-\mathrm{J}_\upsilon(k_{\mathrm{r}2}R_4)\mathrm{Y}_{\upsilon-1}(k_{\mathrm{r}2}R_5)]\,s_{-1,\upsilon}(k_{\mathrm{r}2}R_5)}{\mathrm{J}_\upsilon(k_{\mathrm{r}2}R_4)\mathrm{Y}_\upsilon(k_{\mathrm{r}2}R_5)-\mathrm{J}_\upsilon(k_{\mathrm{r}2}R_5)\mathrm{Y}_\upsilon(k_{\mathrm{r}2}R_4)}\right.\\
&\quad\left.+\frac{2s_{-1,\upsilon}(k_{\mathrm{r}2}R_4)}{\pi k_{\mathrm{r}2}R_5\,[\mathrm{J}_\upsilon(k_{\mathrm{r}2}R_4)\mathrm{Y}_\upsilon(k_{\mathrm{r}2}R_5)-\mathrm{J}_\upsilon(k_{\mathrm{r}2}R_5)\mathrm{Y}_\upsilon(k_{\mathrm{r}2}R_4)]}\right\}+\frac{F_2}{k_{\mathrm{r}2}R_5},\\
c_1 &= \frac{\varepsilon_{33}^{\mathrm{S}}c_{11}^{\mathrm{E}}c_{11}^{\mathrm{E}}-\varepsilon_{33}^{\mathrm{S}}c_{12}^{\mathrm{E}}c_{12}^{\mathrm{E}}+2e_{31}e_{31}c_{11}^{\mathrm{E}}-2e_{31}e_{31}c_{12}^{\mathrm{E}}}{\varepsilon_{33}^{\mathrm{S}}c_{11}^{\mathrm{E}}+e_{31}e_{31}},\quad c_2=\frac{\varepsilon_{33}^{\mathrm{S}}c_{11}^{\mathrm{E}}c_{13}^{\mathrm{E}}-\varepsilon_{33}^{\mathrm{S}}c_{12}^{\mathrm{E}}c_{13}^{\mathrm{E}}+e_{31}e_{33}c_{11}^{\mathrm{E}}-e_{31}e_{33}c_{12}^{\mathrm{E}}}{\varepsilon_{33}^{\mathrm{S}}c_{11}^{\mathrm{E}}+e_{31}e_{31}},\\
c_3 &= \frac{\varepsilon_{33}^{\mathrm{S}}c_{11}^{\mathrm{E}}c_{33}^{\mathrm{E}}-\varepsilon_{33}^{\mathrm{S}}c_{13}^{\mathrm{E}}c_{13}^{\mathrm{E}}+e_{31}e_{31}c_{13}^{\mathrm{E}}+e_{33}e_{33}c_{11}^{\mathrm{E}}}{\varepsilon_{33}^{\mathrm{S}}c_{11}^{\mathrm{E}}+e_{31}e_{31}},\\
t &= \frac{\mathrm{J}_\upsilon(k_{\mathrm{r}1}R_2)\mathrm{Y}_\upsilon(k_{\mathrm{r}1}R_3)-\mathrm{J}_\upsilon(k_{\mathrm{r}1}R_3)\mathrm{Y}_\upsilon(k_{\mathrm{r}1}R_2)}{p},\quad t_0=\frac{\mathrm{J}_\upsilon(k_{\mathrm{r}2}R_4)\mathrm{Y}_\upsilon(k_{\mathrm{r}2}R_5)-\mathrm{J}_\upsilon(k_{\mathrm{r}2}R_5)\mathrm{Y}_\upsilon(k_{\mathrm{r}2}R_4)}{p_0},\\
p &= [\mathrm{J}_\upsilon(k_{\mathrm{r}1}R_2)\mathrm{Y}_\upsilon(k_{\mathrm{r}1}R_3)-\mathrm{J}_\upsilon(k_{\mathrm{r}1}R_3)\mathrm{Y}_\upsilon(k_{\mathrm{r}1}R_2)]\\
&\quad\times\left\{\frac{F_1F_1'(H_{R_3}-H_{R_2})}{2\upsilon^2(4-\upsilon^2)}+F_2F_1'\,[s_{-1,\upsilon}(k_{\mathrm{r}1}R_3)-s_{-1,\upsilon}(k_{\mathrm{r}1}R_2)]+\left(\frac{c_{11}^{\mathrm{E}}}{\varepsilon_{33}^{\mathrm{S}}c_{11}^{\mathrm{E}}+e_{31}e_{31}}-\frac{F_1F_1'}{\upsilon^2}\right)(\ln R_3-\ln R_2)\right\}\\
&\quad+\left[F_1'\mathrm{Y}_\upsilon(k_{\mathrm{r}1}R_2)s_{-1,\upsilon}(k_{\mathrm{r}1}R_3)-F_1'\mathrm{Y}_\upsilon(k_{\mathrm{r}1}R_3)s_{-1,\upsilon}(k_{\mathrm{r}1}R_2)\right]\\
&\quad\times\left\{F_1\left[(\upsilon-2)(J1_{R_3}-J1_{R_2})+J2_{R_2}-J2_{R_3}\right]+F_2\,[\mathrm{J}_\upsilon(k_{\mathrm{r}1}R_3)-\mathrm{J}_\upsilon(k_{\mathrm{r}1}R_2)]\right\}\\
&\quad+\left[F_1'\mathrm{J}_\upsilon(k_{\mathrm{r}1}R_3)s_{-1,\upsilon}(k_{\mathrm{r}1}R_2)-F_1'\mathrm{J}_\upsilon(k_{\mathrm{r}1}R_2)s_{-1,\upsilon}(k_{\mathrm{r}1}R_3)\right]\\
&\quad\times\left\{F_1\left[(\upsilon-2)(Y1_{R_3}-Y1_{R_2})+Y2_{R_2}-Y2_{R_3}\right]+F_2\,[\mathrm{Y}_\upsilon(k_{\mathrm{r}1}R_3)-\mathrm{Y}_\upsilon(k_{\mathrm{r}1}R_2)]\right\},\\
p_0 &= [\mathrm{J}_\upsilon(k_{\mathrm{r}2}R_4)\mathrm{Y}_\upsilon(k_{\mathrm{r}2}R_5)-\mathrm{J}_\upsilon(k_{\mathrm{r}2}R_5)\mathrm{Y}_\upsilon(k_{\mathrm{r}2}R_4)]\\
&\quad\times\left\{\frac{F_1F_1'(H_{R_5}-H_{R_4})}{2\upsilon^2(4-\upsilon^2)}+F_2F_1'\,[s_{-1,\upsilon}(k_{\mathrm{r}2}R_5)-s_{-1,\upsilon}(k_{\mathrm{r}2}R_4)]+\left(\frac{c_{11}^{\mathrm{E}}}{\varepsilon_{33}^{\mathrm{S}}c_{11}^{\mathrm{E}}+e_{31}e_{31}}-\frac{F_1F_1'}{\upsilon^2}\right)(\ln R_5-\ln R_4)\right\}\\
&\quad+\left[F_1'\mathrm{Y}_\upsilon(k_{\mathrm{r}2}R_4)s_{-1,\upsilon}(k_{\mathrm{r}2}R_5)-F_1'\mathrm{Y}_\upsilon(k_{\mathrm{r}2}R_5)s_{-1,\upsilon}(k_{\mathrm{r}2}R_4)\right]\\
&\quad\times\left\{F_1\left[(\upsilon-2)(J1_{R_5}-J1_{R_4})+J2_{R_4}-J2_{R_5}\right]+F_2\,[\mathrm{J}_\upsilon(k_{\mathrm{r}2}R_5)-\mathrm{J}_\upsilon(k_{\mathrm{r}2}R_4)]\right\}\\
&\quad+\left[F_1'\mathrm{J}_\upsilon(k_{\mathrm{r}2}R_5)s_{-1,\upsilon}(k_{\mathrm{r}2}R_4)-F_1'\mathrm{J}_\upsilon(k_{\mathrm{r}2}R_4)s_{-1,\upsilon}(k_{\mathrm{r}2}R_5)\right]\\
&\quad\times\left\{F_1\left[(\upsilon-2)(Y1_{R_5}-Y1_{R_4})+Y2_{R_4}-Y2_{R_5}\right]+F_2\,[\mathrm{Y}_\upsilon(k_{\mathrm{r}2}R_5)-\mathrm{Y}_\upsilon(k_{\mathrm{r}2}R_4)]\right\},
\end{aligned}
$$

where $s_{u,\upsilon}(k_{\mathrm{r}\gamma}r)$ is Rommel function,

$$
\begin{aligned}
&\upsilon=\sqrt{c_1/c_3},\quad F_1=\frac{e_{31}c_{12}^{\mathrm{E}}-e_{31}c_{11}^{\mathrm{E}}}{\varepsilon_{33}^{\mathrm{S}}c_{11}^{\mathrm{E}}+e_{31}e_{31}},\quad F_2=\frac{e_{31}c_{13}^{\mathrm{E}}-e_{33}c_{11}^{\mathrm{E}}}{\varepsilon_{33}^{\mathrm{S}}c_{11}^{\mathrm{E}}+e_{31}e_{31}},\quad F_1'=\frac{F_1}{c_3},\\
&\mathrm{J}1_r=k_{\mathrm{r}\gamma}r\mathrm{J}_\upsilon(k_{\mathrm{r}\gamma}r)s_{-2,\upsilon-1}(k_{\mathrm{r}\gamma}r),\quad \mathrm{Y}1_r=k_{\mathrm{r}\gamma}r\mathrm{Y}_\upsilon(k_{\mathrm{r}\gamma}r)s_{-2,\upsilon-1}(k_{\mathrm{r}\gamma}r),\\
&\mathrm{J}2_r=k_{\mathrm{r}\gamma}r\mathrm{J}_{\upsilon-1}(k_{\mathrm{r}\gamma}r)s_{-1,\upsilon}(k_{\mathrm{r}\gamma}r),\quad \mathrm{Y}2_r=k_{\mathrm{r}\gamma}r\mathrm{Y}_{\upsilon-1}(k_{\mathrm{r}\gamma}r)s_{-1,\upsilon}(k_{\mathrm{r}\gamma}r),\\
&H(r)=(k_{\mathrm{r}\gamma})^2{}_2F_3\left([1,1],\left[2,2+\frac{\upsilon}{2},2-\frac{\upsilon}{2}\right],-\frac{1}{4}(k_{\mathrm{r}\gamma})^2\right).
\end{aligned}
$$

References

[1] Mazue G, Viennet R, Hihn J Y and Albaina D I 2011 *Ultrason. Sonochem.* **18** 895

[2] Guney M and Eskinat E 2007 *Smart Mater. Struct.* **16** 541

[3] Yuan X, Li C, Geng H, Zhai S and Xu L 2017 *J. Test. Eval.* **45** 1396

[4] Kluk P and Milewski A 2015 *Acta Phys. Pol. A* **127** 719

[5] Jia L Y, Zhang G B, Zhang X F, Yao Y and Lin S Y 2017 *Ultrasonics* **74** 204

[6] Chen Z Y, Qian X J, Song X, Jiang Q G, Huang R J, Yang Y, Li R Z, Shung K, Chen Y and Zhou Q F 2019 *Micromachine* **10** 1

[7] Tamano S, Azuma T, Imoto H, Takagi S, Umemura S I and Matsumoto Y 2015 *Jpn. J. Appl. Phys.* **54** 07

[8] Hegde V, Yellampalli S S and Ravikumar H M 2019 *Microsyst. Technol.* **26** 1613

[9] Chilibon I 2003 *Proceedings of the Tenth International Congress on Sound and Vibration Tenth International Congress on Sound & Vibration* July 7–10, 2003, Stockholm, Sweden, p. 1035

[10] Li X and Yao Z 2016 *Smart Mater. Struct.* **25** 075026

[11] Ke Q Q, Liew W H, Zhang L, Tan C K I and Yao Kui 2019 *IEEE Trans. Ultrason. Ferroelectr. Freq. Control.* **67** 968

[12] Wei X Y, Yang Y, Yao W Q and Zhang L 2017 *Sensors* **17** 2253

[13] Mancic D D and Stancic G Z 2010 *J. Sandw. Struct. Mater.* **12** 63

[14] Zhou G, Zhang Y and Zhang B 2002 *Ultrasonics* **40** 907

[15] Kim T, Cui Z, Chang W Y, Kim H, Zhu Y and Jiang X N 2020 *IEEE Trans. Ind. Electron.* **67** 6955

[16] Cannata J M Ritter T A Chen W H Silverman R H and Shung K K 2003 *IEEE Trans. Ultrason. Ferroelectr. Freq. Control.* **50** 1548

[17] Abdullah A, Shahini M and Pak A 2009 *J. Electroceram.* **22** 369

[18] Lin S Y, Fu Z Q, Zhang X L, Wang Y and Hu J 2012 *Smart Mater. Struct.* **22** 015005

[19] Lin S Y, Wang S J and Fu Z Q 2012 *Sens. Actuator A-Phys.* **180** 87

[20] Xu J and Lin S Y 2019 *Sens. Actuator A-Phys.* **286** 133

[21] Xu J and Lin S Y 2019 *J. Acoust. Soc. Am.* **145** 1303

[22] Li G, Gong J H, Wang T, Qiu C R and Xu Z 2018 *Ceram. Int.* **44** S250

[23] Choi H 2019 *Sens. Actuator A-Phys.* **299** 1

[24] Wang J J and Shi Z F 2016 *J. Intell. Mater. Syst. Struct.* **27** 500